

AS-ITP-95-23

July, 1995

Implications on two Higgs doublet models from the latest $b \rightarrow s\gamma$ measurement and top discovery

Chao-Hsi Chang¹ and Caidian Lü²

CCAST (World Laboratory), P.O.Box 8730, Beijing 100080, China,
and

Institute of Theoretical Physics, Academia Sinica, P.O.Box 2735, Beijing 100080, China.³

Abstract

The constraints on the two Higgs doublet model from the new experimental bounds of $b \rightarrow s\gamma$ by CLEO and the latest published value of the top quark mass by CDF and D0 are reanalyzed with the effective Lagrangian covering the full QCD corrections from the energy scale of top quark to that of bottom. The reanalysis result shows that the constraints become more stringent than that of the earlier analysis, i.e. a bigger region of the parameter space of the model is ruled out.

PACS number(s):14.80.Cp, 12.60.Fr, 12.38.Bx

¹ E-mail: zhangzx@itp.ac.cn.

² E-mail: lucd@itp.ac.cn.

³Mailing address.

It is known that the experimental bounds of $b \rightarrow s\gamma$ set very strong constraints on the two Higgs doublet model (2HDM), a minimal extension of the Standard Model (SM). In addition to searching for the neutral Higgs of minimal SM, phenomenologically to investigate possible extensions of SM is also another hot topic in particle physics, thus to apply the latest experimental results of the measurement on $b \rightarrow s\gamma$ [1] and the newly discovery of top quark[2] to reexamine the constraints on the 2HDM so as to upgrade the allowed values of the model parameters is no doubt always to be interesting.

Reviewing the earlier analysis[3], one would find that the QCD correction effects owing to the change of the energy scale from top quark's down to that of W boson were ignored. Indeed this piece of QCD correction itself is not great, but we treat them seriously, and finally find it being not negligible since this correction affects the constraints on the two Higgs doublet model sizable in the report.

Let us first recall the necessary formulas here for later use (mainly from ref.[4]). There are two models for 2HDM to avoid tree-level flavor changing neutral currents (FCNCs). The first (Model I) is to allow only one of the two Higgs doublets to couple to both types, u-type and d-type, of quarks[5] but the other doublet is totally forbidden by certain discrete symmetry. The second (Model II) is to arrange as that one Higgs doublet couples to u-type quarks while the other couples to d-type quarks respectively due to a different discrete symmetry[6]. It is of interest to note that the Model II, as a natural feature, occurs in such a theory as that with supersymmetry or with a Peccei-Quinn type of symmetry.

The piece of the 2HDM Lagrangian for the charged Higgs to the quarks is

$$\begin{aligned} \mathcal{L} = & \frac{1}{\sqrt{2}} \frac{\mu^{\epsilon/2} g_2}{M_W} \left[\left(\frac{v_2}{v_1} \right) \left(\begin{array}{ccc} \bar{u} & \bar{c} & \bar{t} \end{array} \right)_R M_U V \begin{pmatrix} d \\ s \\ b \end{pmatrix}_L - \xi \left(\begin{array}{ccc} \bar{u} & \bar{c} & \bar{t} \end{array} \right)_L V M_D \begin{pmatrix} d \\ s \\ b \end{pmatrix}_R \right] H^+ \\ & + h.c. \end{aligned} \quad (1)$$

where V represents the 3×3 unitary Cabibbo-Kobayashi-Maskawa (CKM) matrix, M_U and M_D denote the diagonalized quark mass matrices, the subscript L and R denote left-handed and right-handed quarks, respectively. For Model I, $\xi = v_2/v_1$; while for Model II, $\xi = -v_1/v_2$. And v_1 , v_2 are the magnitude of the vacuum expectation values of two Higgs doublets, respectively.

The relevant effective Hamiltonian after integrating out the heavy top freedom is:

$$\mathcal{H}_{eff} = 2\sqrt{2}G_F V_{tb} V_{ts}^* \sum_i C_i(\mu) O_i(\mu). \quad (2)$$

The coefficients $C_i(m_t)$ can be calculated from matching conditions at $\mu = m_t$, and $C_i(\mu)$ can be obtained from their renormalization group equation(RGE):

$$\mu \frac{d}{d\mu} C_i(\mu) = \sum_j (\gamma^\tau)_{ij} C_j(\mu), \quad (3)$$

where $(\gamma^\tau)_{ij}$ is the anomalous dimension matrix of the operators O_i . If integrating out the W boson freedom further, once more six relevant four-quark operators will be added[4]. We do not repeat all the operators here but only write down the most relevant operators:

$$\begin{aligned} O_7 &= (e/16\pi^2)m_b \bar{s}_L \sigma^{\mu\nu} b_R F_{\mu\nu}, \\ O_8 &= (g/16\pi^2)m_b \bar{s}_L \sigma^{\mu\nu} T^a b_R G_{\mu\nu}^a. \end{aligned} \quad (4)$$

The effective Hamiltonian appears just below the W -scale as

$$\begin{aligned} \mathcal{H}_{eff} &= \frac{4G_F}{\sqrt{2}} V_{tb} V_{ts}^* \sum_i C_i(M_W) O_i(M_W) \\ &\xrightarrow{EOM} \frac{4G_F}{\sqrt{2}} V_{tb} V_{ts}^* \left\{ \sum_{i=1}^6 C_i(M_W) O_i + C_7(M_W) O_7 + C_8(M_W) O_8 \right\}. \end{aligned} \quad (5)$$

For completeness, the explicit expressions of the coefficient of operators at $\mu = M_W$ are given[4],

$$C_i(M_W) = 0, \quad \text{for } i = 1, 3, 4, 5, 6; \quad C_2(M_W) = 1,$$

$$\begin{aligned} C_{O_8}(M_W) &= \left(\frac{\alpha_s(m_t)}{\alpha_s(M_W)} \right)^{\frac{14}{23}} \left\{ \frac{1}{2} C_{O_{LR}^1}(m_t) - C_{O_{LR}^2}(m_t) + \frac{1}{2} C_{P_L^{1,1}}(m_t) \right. \\ &\quad \left. + \frac{1}{4} C_{P_L^{1,2}}(m_t) - \frac{1}{4} C_{P_L^{1,4}}(m_t) \right\} - \frac{1}{3}, \end{aligned} \quad (6)$$

$$\begin{aligned} C_{O_7}(M_W) &= \frac{1}{3} \left(\frac{\alpha_s(m_t)}{\alpha_s(M_W)} \right)^{\frac{16}{23}} \left\{ C_{O_{LR}^3}(m_t) + 8C_{O_{LR}^2}(m_t) \left[1 - \left(\frac{\alpha_s(M_W)}{\alpha_s(m_t)} \right)^{\frac{2}{23}} \right] \right. \\ &\quad + \left[-\frac{9}{2} C_{O_{LR}^1}(m_t) - \frac{9}{2} C_{P_L^{1,1}}(m_t) - \frac{9}{4} C_{P_L^{1,2}}(m_t) + \frac{9}{4} C_{P_L^{1,4}}(m_t) \right] \left[1 - \frac{8}{9} \left(\frac{\alpha_s(M_W)}{\alpha_s(m_t)} \right)^{\frac{2}{23}} \right] \\ &\quad \left. - \frac{1}{4} C_{P_L^4}(m_t) + \frac{9}{23} 16\pi^2 C_{W_L^1}(m_t) \left[1 - \frac{\alpha_s(m_t)}{\alpha_s(M_W)} \right] \right\} - \frac{23}{36}, \end{aligned} \quad (7)$$

and together with the coefficients of operators at $\mu = m_t$,

$$C_{W_L^1} = \delta/g_3^2,$$

$$\begin{aligned} C_{O_{LR}^1} &= - \left(\frac{1+\delta}{2(1-\delta)^2} + \frac{\delta}{(1-\delta)^3} \log \delta \right) - \xi' \left(\frac{1+x}{2(1-x)^2} + \frac{x}{(1-x)^3} \log x \right), \\ C_{O_{LR}^2} &= - \frac{1}{2} \left(\frac{1}{(1-\delta)} + \frac{\delta}{(1-\delta)^2} \log \delta \right) - \xi' \left(\frac{1}{2(1-x)} + \frac{x}{2(1-x)^2} \log x \right), \end{aligned}$$

$$\begin{aligned}
C_{O_{LR}^3} &= \left(\frac{1}{(1-\delta)} + \frac{\delta}{(1-\delta)^2} \log \delta \right) + \xi \left(\frac{1}{1-x} + \frac{x}{(1-x)^2} \log x \right), \\
C_{P_L^{1,1}} &= C_{P_L^{1,3}} = \left(\frac{\frac{11}{18} + \frac{5}{6}\delta - \frac{2}{3}\delta^2 + \frac{2}{9}\delta^3}{(1-\delta)^3} + \frac{\delta + \delta^2 - \frac{5}{3}\delta^3 + \frac{2}{3}\delta^4}{(1-\delta)^4} \log \delta \right) \\
&\quad + \left(\frac{v_2}{v_1} \right)^2 \left(\frac{\frac{11}{18} - \frac{7}{18}x + \frac{1}{9}x^2}{(1-x)^3} + \frac{x - x^2 + \frac{1}{3}x^3}{(1-x)^4} \log x \right), \\
C_{P_L^{1,2}} &= \left(\frac{-\frac{8}{9} - \frac{1}{6}\delta + \frac{17}{6}\delta^2 - \frac{7}{9}\delta^3}{(1-\delta)^3} + \frac{-\delta + \frac{10}{3}\delta^3 - \frac{4}{3}\delta^4}{(1-\delta)^4} \log \delta \right) \\
&\quad + \left(\frac{v_2}{v_1} \right)^2 \left(\frac{-\frac{8}{9} + \frac{29}{18}x - \frac{7}{18}x^2}{(1-x)^3} + \frac{-x + 2x^2 - \frac{2}{3}x^3}{(1-x)^4} \log x \right), \\
C_{P_L^{1,4}} &= \left(\frac{\frac{1}{2} - \delta - \frac{1}{2}\delta^2 + \delta^3}{(1-\delta)^3} + \frac{\delta - 3\delta^2 + 2\delta^3}{(1-\delta)^4} \log \delta \right) \\
&\quad + \left(\frac{v_2}{v_1} \right)^2 \left(\frac{1 - x^2}{2(1-x)^3} + \frac{x - x^2}{(1-x)^4} \log x \right), \\
C_{P_L^4} &= \frac{1}{Q_b} \left(\frac{-\frac{1}{2} - 5\delta + \frac{17}{2}\delta^2 - 3\delta^3}{(1-\delta)^3} + \frac{-5\delta + 7\delta^2 - 2\delta^3}{(1-\delta)^4} \log \delta + 4\delta \log \delta \right) \\
&\quad - \frac{1}{Q_b} \left(\frac{v_2}{v_1} \right)^2 \left(\frac{1 - x^2}{2(1-x)^3} + \frac{x - x^2}{(1-x)^4} \log x \right). \tag{8}
\end{aligned}$$

Where $\delta = M_W^2/m_t^2$, $x = m_\phi^2/m_t^2$; With

$$\xi' = v_2^2/v_1^2, \quad \text{Model I},$$

$$\xi' = -1, \quad \text{Model II}.$$

When $\xi = \xi' = 0$, the above result (8) reduces to that of SM case[7].

The running of the coefficients of operators from $\mu = M_W$ to $\mu = m_b$ was well described in refs.[8, 9, 10, 11, 12, 13]. With the running due to QCD, the coefficients of the operators at $\mu = m_b$ scale:

$$C_7^{eff}(m_b) = \eta^{16/23} C_7(M_W) + \frac{8}{3}(\eta^{14/23} - \eta^{16/23}) C_8(M_W) + C_2(M_W) \sum_{i=1}^8 h_i \eta^{a_i}. \tag{9}$$

Here $\eta = \alpha_s(M_W)/\alpha_s(m_b)$,

$$h_i = \left(\frac{626126}{272277}, -\frac{56281}{51730}, -\frac{3}{7}, -\frac{1}{14}, -0.6494, -0.0380, -0.0186, -0.0057 \right),$$

$$a_i = \left(\frac{14}{23}, \frac{16}{23}, \frac{6}{23}, -\frac{12}{23}, 0.4086, -0.4230, -0.8994, 0.1456 \right).$$

Following refs.[8, 9, 11, 12, 13],

$$BR(B \rightarrow X_s \gamma)/BR(B \rightarrow X_c e \bar{\nu}) \simeq \Gamma(b \rightarrow s \gamma)/\Gamma(b \rightarrow c e \bar{\nu}). \tag{10}$$

Then

$$\frac{BR(B \rightarrow X_s \gamma)}{BR(B \rightarrow X_c e \bar{\nu})} \simeq \frac{|V_{ts}^* V_{tb}|^2}{|V_{cb}|^2} \frac{6\alpha_{QED}}{\pi g(m_c/m_b)} |C_7^{eff}(m_b)|^2, \quad (11)$$

where the phase space factor $g(z)$ is given by:

$$g(z) = 1 - 8z^2 + 8z^6 - z^8 - 24z^4 \log z, \quad (12)$$

here we use $m_c/m_b = 0.316$. Afterwards one obtains the $B \rightarrow X_s \gamma$ decay rate normalized to the quite well established semileptonic decay rate $Br(B \rightarrow X_c e \bar{\nu})$. If we take experimental result $BR(B \rightarrow X_c e \bar{\nu}) = 10.8\%$ [14], the branching ratios of $B \rightarrow X_s \gamma$ is found to be:

$$BR(B \rightarrow X_s \gamma) \simeq 10.8\% \times \frac{|V_{ts}^* V_{tb}|^2}{|V_{cb}|^2} \frac{6\alpha_{QED}}{\pi g(m_c/m_b)} |C_7^{eff}(m_b)|^2. \quad (13)$$

Note that in the above equations the top mass m_t is kept as a parameter precisely thus we may apply them to computing all the values with various experimental m_t as one needs.

To emphasize the consequences have been ignored in literature, first of all we plot the coefficients of the most relevant operators O_7 and O_8 at $\mu = M_W$ versus $\tan \beta$ with and without the QCD corrections of the energy scale running from m_t (with the latest experimental value) to M_W in Fig.1 for Model I and Model II respectively. Here $m_b = 4.8\text{GeV}$, $M_W = 80.22\text{GeV}$ and the QCD coupling $\alpha_s(m_Z) = 0.125$ are taken[14]. Owing to the mixing of all the relevant operators being small, one may see the fact that the effects of the QCD corrections are roughly within ten percent and not depend on $\tan \beta$ very much. However, one will see soon that the effects, though only in ten percent, will make substantial changes for the constraints on the parameter space of 2HDM. In order to see the experimental uncertainties of the measurements of the branching ratio $BR(b \rightarrow s\gamma)$, the top mass m_t and the strong coupling constant $\alpha_s(M_Z^2)$ how to affect the conclusions, we plot the branching ratio $BR(b \rightarrow s\gamma)$ (the central value also with three standard deviation upper and lower bounds achieved by CLEO recently) versus $\tan \beta$ so as to show the constraints on $\tan \beta$ and on the mass of charged Higgs M_ϕ for Model I (Fig.2a) and Model II (Fig.2b), and plot the bands in the parameter space $\tan \beta$ versus M_ϕ to show the constraints caused by taking $m_t = 176\text{GeV}$ with $\alpha_s(M_Z^2) = 0.12$ and 0.13 (the dashed lines) and $\alpha_s(M_Z^2) = 0.125$ with $m_t = 163\text{GeV}$ and 189GeV (the solid lines) for Model I (Fig.3a) and Model II (Fig.3b) respectively. Here it is interesting to note that in Fig.3b, the dashed lines approach to 350GeV and 390GeV respectively whereas the solid lines approach to 310GeV and 430GeV respectively when $\tan \beta$ approaches to infinity. All lines in Fig.3, are obtained by taking the 95% C.L. value of CLEO, $1.0 \times 10^{-4} < Br(B \rightarrow X_s \gamma) < 4.2 \times 10^{-4}$ [1]. It is shown that the parameter space is more sensitive for changing of m_t than for α_s , especially in Model II.

One may see from Figs.2a,3a that for Model I, there are two bands in the $\tan \beta$ - M_ϕ plane, excluded by our reanalysis with the latest measurements on $b \rightarrow s + \gamma$

and m_t . Finally, as another result of the reanalysis, in Fig.4 we plot the $\tan\beta$ versus M_ϕ plane to show the excluded region of the parameters for Model II at 95% C.L.. The solid line corresponds to the conclusion of the present analysis with the central values of all the parameters (m_t, α_s and the branching ratio of the semileptonic decay of b quark etc.); the dashed line corresponds to a possible parameter: $|V_{ts}^* V_{tb}|^2 / |V_{cb}|^2 = 0.99$ instead of $|V_{ts}^* V_{tb}|^2 / |V_{cb}|^2 = 0.95$ ⁴; and the dot-dashed line corresponds to the results obtained by other authors[3], which do not include the piece of the QCD corrections from m_t to M_W ,

In conclusion, due to the QCD corrections from m_t to M_W , the new experimental value of m_t and the bounds for $b \rightarrow s\gamma$, the constraints for 2HDM are strained substantially. For instance, the lower bound for the mass of the charged Higgs is put up at least 150GeV for Model II.

Acknowledgements

The work was supported in part by the National Natural Science Foundation of China and the Grant LWTZ-1298 of Chinese Academy of Science. The authors would like to thank Prof. T.D. Lee, the director of CCAST for creating the very active institution in Beijing, since this work actually begins in one of the domestic workshops (April-May, 1995) of CCAST.

References

- [1] M.S.Alam et al., CLEO Collaboration, Phys. Rev. Lett. **71**, 674 (1993), ibid. **74**, 2885 (1995).
- [2] F. Abe et al., CDF Collaboration, Phys. Rev. Lett. **74**, 2626 (1995); S. Abachi et al., D0 Collaboration, Phys. Rev. Lett. **74**, 2632 (1995).

⁴This value is widely adopted for all the earlier analysis. In fact, there are uncertainties from the measurements and the formulars on the branching ratio of the inclusive semileptonic decay of B meson $BR(B \rightarrow X_c e\bar{\nu})$ (see eq.(11)) as well as those from the determination of the CKM matrix elements. Concerning the facts of the uncertainties and the possibility for more than three generations of the elementary fermions, we try to change the value of $|V_{ts}^* V_{tb}|^2 / |V_{cb}|^2$, so as to let one see the tendency for the constraints when the value becomes greater (equivalent to that the value of $BR(B \rightarrow X_c e\bar{\nu})$ becomes smaller than 10.8% etc. .

- [3] A.J. Buras, M. Misiak, M. Münz and S. Pokorski, Nucl. Phys. **B424**, 374 (1994); M. Ciuchini et al. Phys. Lett. **B334** 137 (1994); A.K. Grant, Phys. Rev. **D51**, 207 (1995); G.T. Park, preprint YUMS-95-9, SNUTP-95-030, hep-ph/9504369.
- [4] C.D. Lü, Nucl. Phys. **B441** (1995) 33.
- [5] H.E. Haber, G.L. Kane and T. Sterling, Nucl. Phys. **B161** (1979) 493.
- [6] S.L. Glashow and S. Weinberg, Phys. Rev. **D15** (1977) 1958.
- [7] C.S. Gao, J.L. Hu, C.D. Lü and Z.M. Qiu, preprint CCAST-93-28, hep-ph/9408351, to appear in Phys. Rev. D.
- [8] B. Grinstein, R. Springer and M.B. Wise, Phys. Lett. **B202**, 138(1988); Nucl. Phys. **B339**, 269 (1990).
- [9] R. Grigjanis, P.J. O'Donnell, M. Sutherland, H. Navelet, Phys. Lett. **B213**, 355 (1988); ibid. **B286** 413(E);
- [10] G. Celli, G. Curci, G. Ricciardi, A. Vicere, Phys. Lett. **B248**, 181 (1990); ibid. **B325**, 227 (1994).
- [11] M. Misiak, Phys. Lett. **B269**, 161 (1991); Nucl. Phys. **B393**, 23 (1993).
- [12] K. Adel and Y.P. Yao, Mod. Phys. Lett. A8 (1993) 1679.
- [13] M. Ciuchini, E. Franco, G. Martinelli, L. Reina, L. Silvestrini, Phys. Lett. **B316**, 127(1993); M. Ciuchini, E. Franco, L. Reina, L. Silvestrini, Nucl. Phys. **B421**, 41 (1994).
- [14] Particle Data Group, Phys. Rev. **D45** (1992) No.11.

Figure Captions

1. Coefficients of operators O_7 , O_8 , as functions of $\tan \beta$ in Model I (a) and Model II (b). Solid and dashed lines correspond to C_7 with and without QCD running from m_t to M_W ; dash-dotted and dotted lines correspond to C_8 with and without QCD running from m_t to M_W .
2. Branching ratios of $b \rightarrow s\gamma$ depicted as functions of $\tan \beta$, with different masses of the charged Higgs M_ϕ in Model I (a), and Model II (b). The CLEO experiment's central value, upper and lower limit of 95% C.L. for this decay are also depicted as solid lines.
3. $\tan \beta$ - M_ϕ plane to show excluded region of parameters of Model I (a), Model II (b). Every two solid lines denote the allowed and excluded region(s) with $\alpha_s(m_Z) = 0.125$ and $m_{top} = 189GeV$ or $m_{top} = 163GeV$; Every two dashed lines correspond to that of $m_{top}=176GeV$ and $\alpha_s(m_Z) = 0.13$ or $\alpha_s(m_Z) = 0.12$.
4. $\tan \beta$ - M_ϕ plane to show excluded region of parameters of Model II. Solid lines corresponds to all central value of parameters; dashed line correspond to $|V_{ts}^*V_{tb}|^2/|V_{cb}|^2 = 0.99$; and dot-dashed line correspond to results without QCD Corrections from m_t to M_W , obtained by other authors.

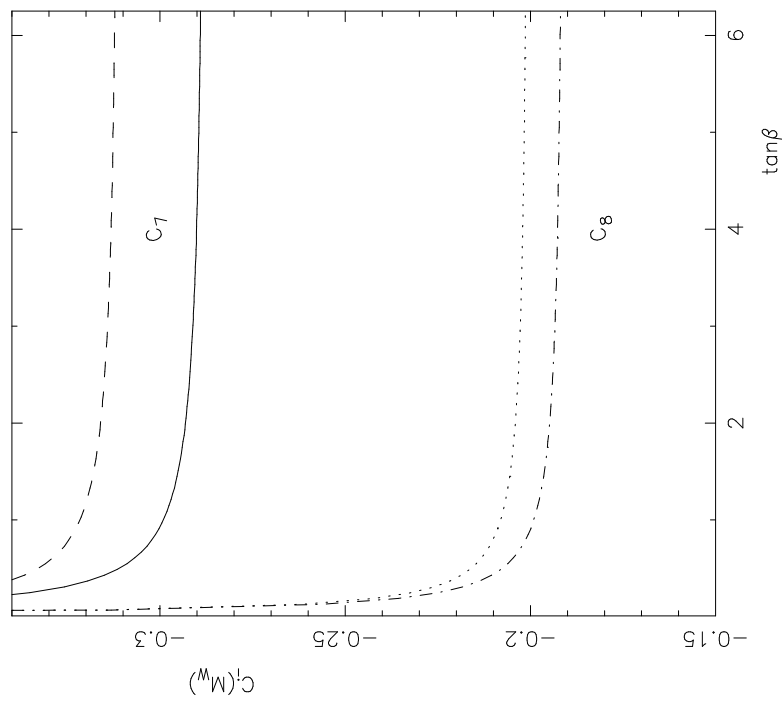


Fig. 1 (b)

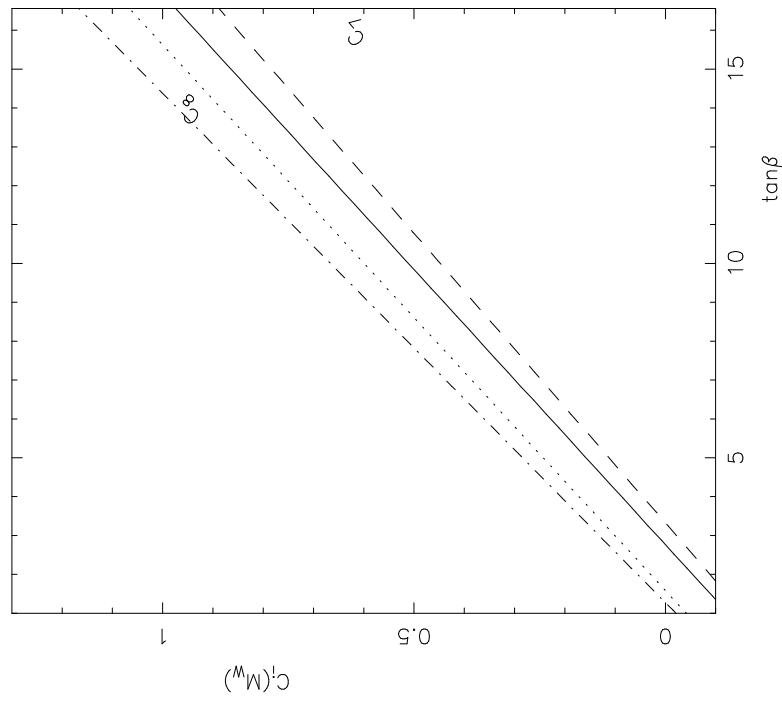


Fig. 1 (a)

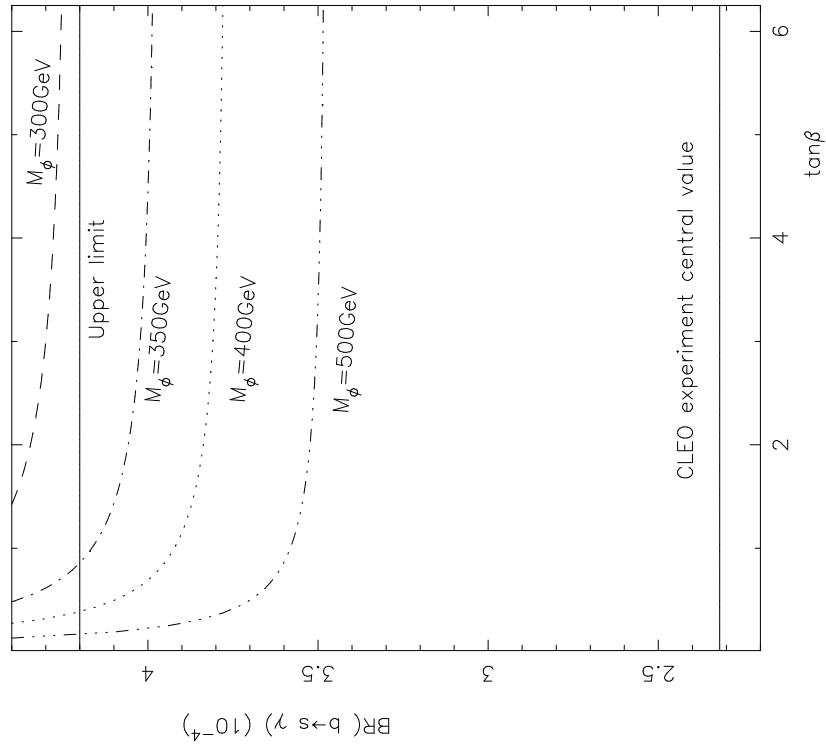


Fig. 2 (a)

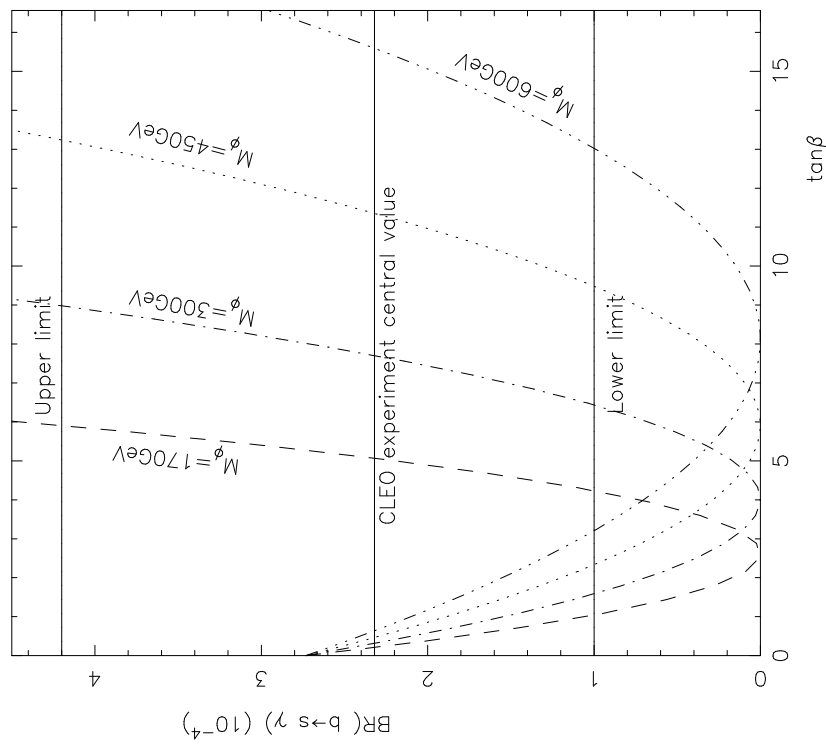


Fig. 2 (a)

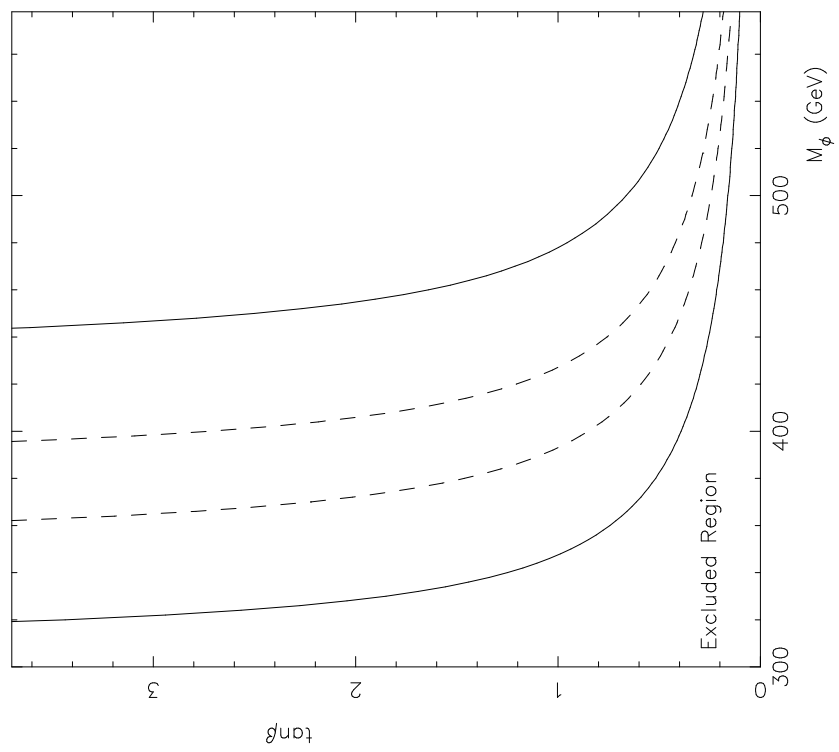


Fig. 3 (b)

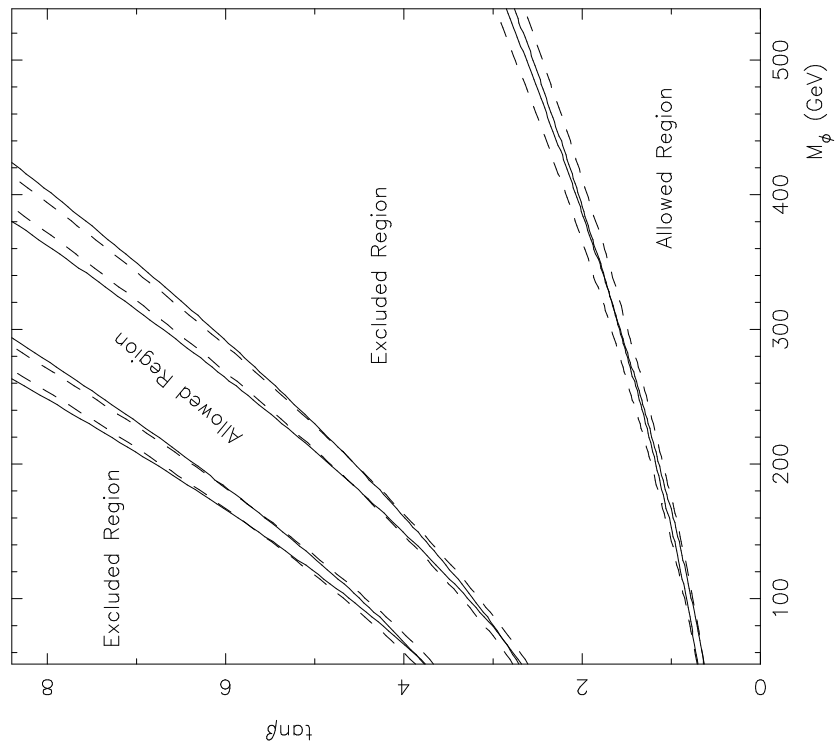


Fig. 3 (a)

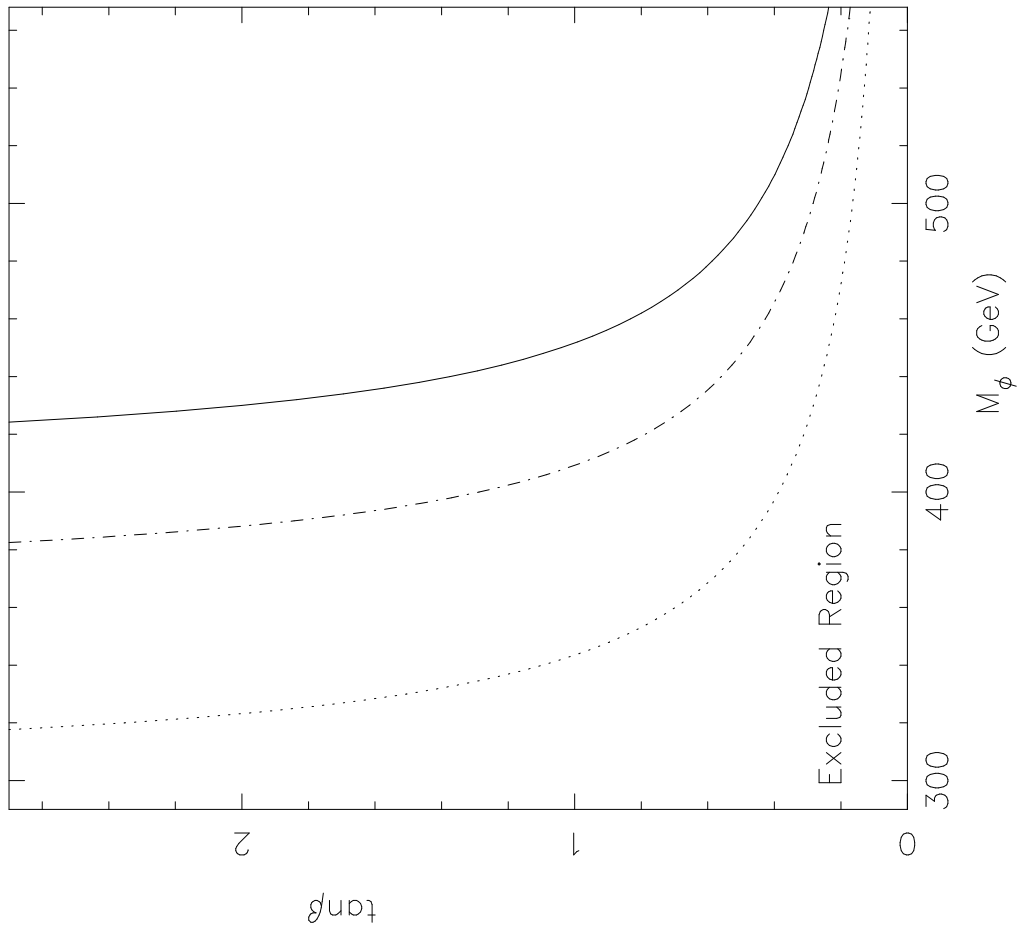


Fig. 4